15

Combining data sets in data analysis with interval uncertainty

© A.N. Bazhenov,[1,2] A.Yu. Telnova[1]

[1] Ioffe Institute,
194021 St. Petersburg, Russia
[2] Peter the Great St. Petersburg Polytechnic University (SPbPU),
Physics and Mechanical Institute,
194064 St. Petersburg, Russia
e-mail: bazhenov_an@spbstu.ru

Received July 1, 2024
Revised November 26, 2024
Accepted November 27, 2024

A practical example of the use of interval statistics methods in the field of nuclear physics is given. It is shown how these methods allow combining two samples in an optimal way. The correction parameter of one of the samples is a multiplicative correction for the background in one of the spectral regions. From physical considerations, the background value estimate is known. The working tool in optimization is a combined measure of consistency, which ensures the receipt of external and internal estimates simultaneously. Optimality in this case implies an increase in the size of the maximum clique in the interval sample. Thus, the volume of data for calculating the constant of the fundamental nuclear reaction increases, which makes the calculation result more reliable. Based on the results of combining the samples, a new value of the physical quantity was calculated, namely, the circular polarization of gamma quanta in the reaction of capture of a polarized neutron by protons.

Keywords: measurement status, fully compatible measurements, Jaccard coefficient, measure of compatibility, interval analysis, interval statistics, covering and non-covering measurements and samples, information set, interval mode.

DOI: 10.61011/TP.2025.04.61221.218-24

Introduction

This paper continues the subject of application of interval analysis and interval statistics for processing a physical experiment [1,2]. The fundamentally methodological issues of the interval statistics are considered in the book [3].

The task of determining the constant value is a basic task of data analysis. The constant magnitude means a value which is invariable during measurements. This category includes the world physical constants, which in today's natural science are considered to be invariable across the entire Universe both in space and time. Thus, the range of applications is extended from the most routine situational measurements to measuring the fundamental characteristics of the matter.

The constant value is evaluated using various measures of the location and scattering. The theory&probability mathematical statistics applies both parametric estimates based on theoretical distributions and non-parametric estimates, for example, the median methods, the Tukey estimates, etc.

In case of interval data, one's own specific methods for sample evaluation are applied [3]. Further, we shortly represent necessary notions of data analysis with interval uncertainty. Then we will consider the task of determining one of the parameters of the nuclear physics basic reaction - radiation capture of neutron by a proton ($np \to d\gamma$). Based on the previously published data, we propose a method of extending the data sample using the structures [1,2].

1. Theoretical foundations of interval analysis

1.1. Basic definitions

The interval analysis is a mathematics section which describes objects by means of intervals. The present work uses definitions, methodology and terminology from [4] and a modern system of designation from [5]. Since the interval arithmetic has real arithmetic as a limit for, it is necessary to distinguish designations of objects of various kinds of the arithmetic in writing. In this regard, all the interval objects - scalars, vectors, matrices, are denoted in bold font [5].

The interval $[a, b]$ of the real axis $\mathbf{R}$ is a set of all the number located between the specified number a, b, including a, b, i.e.:

$$[a, b] := \{x \in \mathbf{R} | a \leq x \leq b\}, \quad (1)$$

while a and b are endpoints of the interval $[a, b]$.

The other basic definitions of the interval analysis are contained in the work [1,2]. The interval analysis is described in detail in the book by S.P. Shary „Finite-dimensional interval analysis“ [4].

We provide necessary information from a relatively new section of data analysis - interval statistics or data analysis with interval uncertainty [3]. The key in this approach includes the notions a covering measurement and a covering sample. The covering measurement means such interval measurement which contains a true value of the measured

quantity. The covering samples will be a sample in which the covering measurements predominate. In practice, it is not always possible to check the covering notion since the true value of the quantity is not often known. For practical purposes, the covering requirements is replaced by the requirement of sample compatibility which is used hereinafter.

1.2. Information set and measurement status

When solving specific problems with samples of the interval data, the most important role is given to the notion of the information set. In accordance with [3], it means a set of values of quantities interesting to us, which are compatible with the measurement data within the selected model of their processing. As applied to the measurement of the constant quantity, compatibility of the data with the model can be expressed as conditions for relationship of the model parameters intervals $\mathbf{\Omega}$ and the interval of the specific measurement $\mathbf{x}_i$. The methods of finding $\mathbf{\Omega}$ may be different (mode, median), while the relationship may be intersections or an inclusion minimum. For the different measurements, the different variants of the relationship of $\mathbf{\Omega}$ and $\mathbf{x}_i$ may occur.

The papers [4,5] introduced the notions which characterize influence of separate measurements on the information set. We will use the terms: internal, external and boundary measurements. In accordance with [4,5], the measurement is internal if it does not change the information set. The internal measurements of xi are compatible with the model of $\mathbf{\Omega}$ and do not contain the boundaries by the model $\delta\mathbf{\Omega}$:

$$\Omega \in x_i, \quad \delta\Omega \notin x_i.$$

Thus, these measurement „cover" the model „with a margin" and their influence on the model is almost zero. The boundary measurement contain at least one boundary of the information set. It is these measurements that for the information set. The external measurements change the information set.

It may seem that the internal measurements are not significant at all, which, in our opinion, is not quite equitable. After considering the practical example, we will additionally discuss the terms of description of a measurement status.

2. Practical example

2.1. Source data

The data on circular polarization of γ-quanta $np \to d\gamma$ with polarized neutrons are important for nuclear physics and nucleosynthesis. The most accurate measurements of the circular polarization which were carried out in the weak interaction laboratory of the academician V.M. Lobashev in RAS PNPI in 1988–1991 are given in the work [6]. The experiment is detailed in the papers [7–10].Specifically,

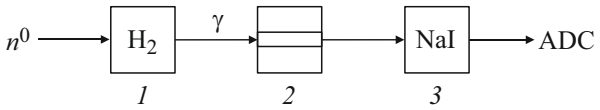

Figure 1. Setup for measuring the circular polarization of gamma-quanta in the reaction$np \to d\gamma$.

the paper [7] represents a system of neutron spin control, while the paper [8] describes a solid parahydrogen target and a unit for production of pure parahydrogen, the paper [9] — describes the experiment recording system and the work [10] — describes a study of influence of the magnetic field on the gamma-quantum detector.

Fig. 1 shows a simplified diagram of the unit for measuring the circular polarization of the gamma-quanta in the reaction $np \to d\gamma$ [7–10]. The beam of cold polarized neutrons of the PWR-M belonging to RAS PNPI was delivered to the solid parahydrogen target *1*. The gamma-quanta of the reaction $np \to d\gamma$ and the energy of 2.22 MeV. The polarization was measured using the analyzer *2* designed as a magnetized ferromagnetic with the absorption length of about 70 mm. The efficiency of the analyzer was about 5%. The gamma quanta were recorded using a scintillation NaI(Tl) detector of the diameter of 150×100 mm. The ADC electron recording system made it possible to record in three energy ranges: in the photopeak of 2.22 MeV, in the high-energy range of Compton scattering and in the background range with the energy above 2.22 MeV.

The theoretical calculations were carried out in terms of nuclear physics [11], which in a wide context discusses deutron physics, and the work [12], which provides details of calculation of the circular polarization, and in terms of nucleosynthesis during the Big Bang [13]. Moreover, thin effects in the deutron structure can affect analysis of precision measurements of A_γ-asymmetry when capturing the nonpolarized neutrons [14,15]. The present experiment uses methods of the works [6,8,9], but with the nonpolarized neutrons.

Measurement of the circular polarization of the γ-quanta is based on dependence of their Compton scattering section on polarization of electrons in the magnetized ferromagnetic. The experimental effect was calculated by the formula (2):

$$\delta_0 = 2\frac{N^+ - N^-}{N^+ + N^-}, \tag{2}$$

where N^+, N^- — counts of the γ-quanta with various polarization of neutrons. The number of the measurements was $N \approx 10^{10}$ in each series, so the statistical error was of the order of $\approx 10^{-5}$.

The experimental data was processed in [6] taking into account about half a data. Table 1 shows a part of the date of [6]. The experiment had no direct capability of measuring the background in the Compton range of the detector-caught quanta with the energy of 2.22 MeV. Moreover, at

Table 1. Data (1) multiplied by 10^5 ((−) the data non included in [6]), RMSD — the root-mean-square deviation

№of the measurement series	Compton — average	Compton — RMSD	Photopeak	Photopeak — RMSD	Background	Background — RMSD
(1)	(2)	(3)	(4)	(5)	(6)	(7)
	x^C	Δx^C	x^p	Δx^p	x^b	Δx^b
1	−3.1	2.7	−4.4	2.7	4.2	6.7
2	−0.2	2.1	−3.4	1.9	−3.2	4.8
3	−4.0	2.1	−6.9	2.4	12.1	9
4	−2.1	2.5	−1.2	2.4	12.4	7.2
5	−3.7	1.9	−1.0	2.7	9.4	5.1
6	−1.7	3.7	−10.8	3.5	1	12.4
7	−5.7	2.8	−10.2	2.8	−0.6	6.1
8	−2.8	1.9	−6.3	2	3.9	4.3
9	−8.0	4.0	−10.4	4.1	10.3	10
10	−2.1	3.9	0.6	3.4	−4.8	10.6
11	−3.6	2.6	−1.8	2	4.6	4.2
12	−7.2	2.5	−6.6	2.1	−5.7	4.6
13	(−)	(−)	−4.9	2.1	13	3
14	(−)	(−)	−6.0	2.4	8.4	4.6
15	(−)	(−)	−4.0	2.7	10.6	5.5
Average	−3.5	0.7	−4.8	0.8	5.8	1.7

that time the calculation capabilities were insufficient for calculation of realistic geometry detectors. This calculation still does not fully resolve the problem due to the fact that the high-energy background appears simultaneously with useful signals because of neutron scattering on the target substance [16].

In the present work, we present the mathematical approach, which together with generalized metrics of compatibility provides the use of a great deal of the experimental data for calculation of the effects.

In order to apply the methods of interval statistics we will form the interval data and their sample. The data in the form of the intervals are derived from the data of the columns 4 and 5 of Table 1 in the form of [3]:

$$\mathbf{x}_i^p = [x_i^p - \Delta x_i^p, x_i^p + \Delta x_i^p]. \qquad (3)$$

The sample of the interval data $\mathbf{X}^p$ (4) consists of the values $\mathbf{x}_i^p$ (3):

$$\mathbf{X}^p = \{\mathbf{x}_i^p\}^n, \quad i = 1, 2, \ldots, n, \quad n = 15. \qquad (4)$$

Relating to the data (3), the band scattering diagram of the sample of the interval data $\mathbf{X}^p$ within the photopeak range and the endpoints of the intervals of the array $\mathbf{Z}$ are shown in Fig. 2.

The sample of the interval data $\mathbf{X}^p$ has no property of compatibility, since in terms of classic interval arithmetic the intersection of all the measurements is empty: $\cap \mathbf{x}_i^p = \varnothing$.

Due to emptiness of intersection of all the measurements, for the information set we will use an interval mode, which

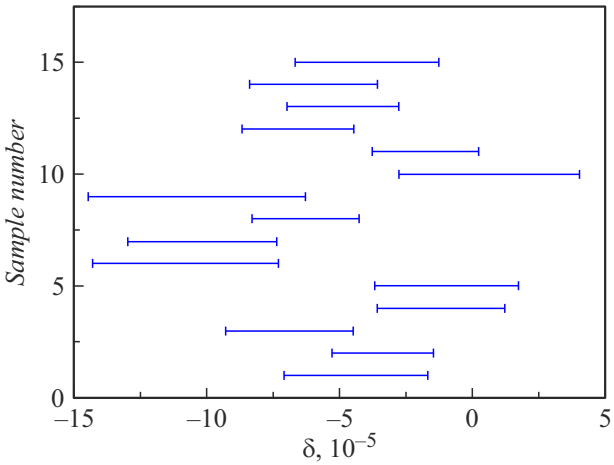

Figure 2. Scattering pattern of the sample of the interval data $\mathbf{X}^p$ and the endpoints of the intervals of the array $\mathbf{Z} = \{\mathbf{z}_i^p\}$ within the photopeak range, as multiplied by 10^5.

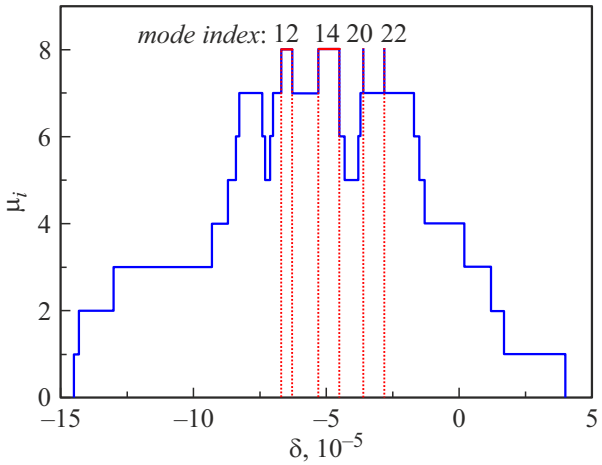

Figure 3. Graph of the frequencies of the elementary subintervals **Z**.

generalizes the common notion of the sample mode in the statistics. In order to calculate the interval mode according to the method of the book [3], it is necessary to create the array of elementary subintervals of measurements of **Z**. It consists of increasingly ordered values of the endpoints of the intervals of the data $\mathbf{x}_i^p = [\underline{x}_i^p, \overline{x}_i^p]$:

$$\mathbf{Z}^p = \{\mathbf{z}_i^p\}^n, \quad i = 1, 2, \ldots, N, \quad N = 2n - 1 = 29. \quad (5)$$

The interval mode is found by calculating the frequencies μ_i of entry of the elementary subintervals to the interval data taking into account the condition (6):

$$\mathbf{z}_i \cap \mathbf{x}_i^p \neq \emptyset, \quad j = 1, 2, \ldots, n, \quad i = 1, 2, \ldots, N. \quad (6)$$

The maximum of the graph μ_i corresponds to the interval mode. The graph of the frequencies μ_i is shown in Fig. 3. The top includes the numbers of the elementary subintervals $\mathbf{z}_i$, which form the mode $\mathbf{X}^p$.

As it is clear from the graph of Fig. 3, the size of the maximum clique is 8 measurements of 15. The distribution mode is a multi-interval (7):

$$\text{mode}\,\mathbf{X}^p = \mathbf{z}_{12} \cup \mathbf{z}_{14} \cup \mathbf{z}_{20} \cup \mathbf{z}_{22} = [-6.7, -6.3]$$
$$\cup [-5.3, -4.5] \cup [-3.6, -3.6] \cup [-2.8, -2.8]. \quad (7)$$

The intervals $\mathbf{z}_{20}$ and $\mathbf{z}_{22}$ are degenerate. This fact is due to a method of data representation in [6] with a low number of significant digits after the decimal dot.

The result of calculations as the multi-interval in the form of (6) makes it difficult to interpret the study result. The following looks more natural

$$\text{mode}\,\mathbf{X}^p = \mathbf{z}_{12} \cup \mathbf{z}_{14} = [-6.7, -6.3] \cup [-5.3, -4.5]. \quad (8)$$

The maximum clique K_p includes 8 measurements

$$K_p = \{1, 3, 8, 9, 12, 13, 14, 15\}, \quad (9)$$

which is just slightly above the half of the sample $\mathbf{X}^p$.

2.2. Additional data and their inclusion in the initial sample

The data representativity was increased by taking measurements within the Compton scattering range, which are included in the columns 2 and 3 of Table 1. They form the sample of interval data $\mathbf{X}^c$ which is formed similar to $\mathbf{X}^p$ (2) by the data of the 1-st and 2-nd columns.

Externally, it is clear from the scattering pattern of the interval data sample $\mathbf{X}^p$ and $\mathbf{X}^c$ of Fig. 4 that the data of the Compton scattering and the photopeak are pair-by-pair compatible for the majority of the measurements. Thus, presumably, they can be quite used in the processing after necessary correction.

Let us set the most simple model of correction. We will believe that the relative background contribution in all the measurements was the constant quantity and the coefficient k_{BG} taking this fact into account can also be considered the constant one. We consider that the true quantity within the Compton scattering

$$x_C = k_{BG} x_{C_0}, \quad (10)$$

where x_C — the corrected data, x_{C_0} — the data of the column 2 of Table 1. After correction of the data $\mathbf{X}_C$, they were included together with the data $\mathbf{X}^p$ (3) into a single interval sample $\mathbf{X} = \{\mathbf{X}^p, \mathbf{X}^c\} = \{\mathbf{X}^p, \mathbf{k}_{BG}\mathbf{X}^{c0}\}$.

The quantity k_{BG} is believed to be unknown. It was determined by the methods for the first time proposed in [1] using the combined measure of compatibility [2]. The point and interval estimates are calculated using one-dimensional optimization within the value range from 1 (no correction) to 2 (very rough estimate of the background). The estimate by the Jaccard index provides the point estimate argument.

$$k_{BG}^{opt} = \text{argmax}_{k_{BG}}\, Ji. \quad (11)$$

The interval estimate is determined by values of the Oskorbin coefficient k_O and the maximum frequency $\max \mu_i$.

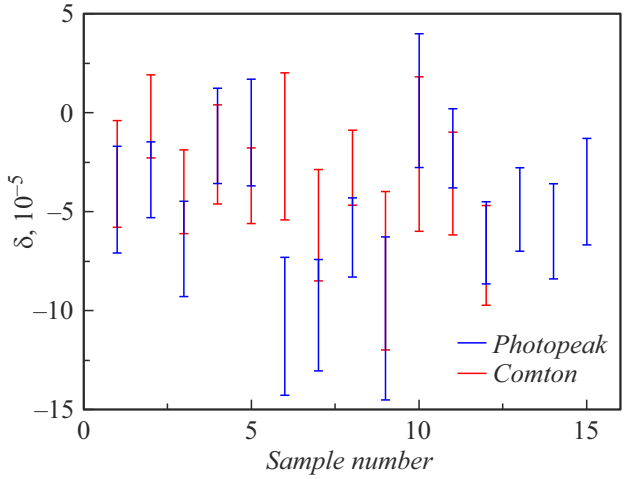

Figure 4. Scattering pattern of the interval data sample $\mathbf{X}^p$ and $\mathbf{X}^c$.

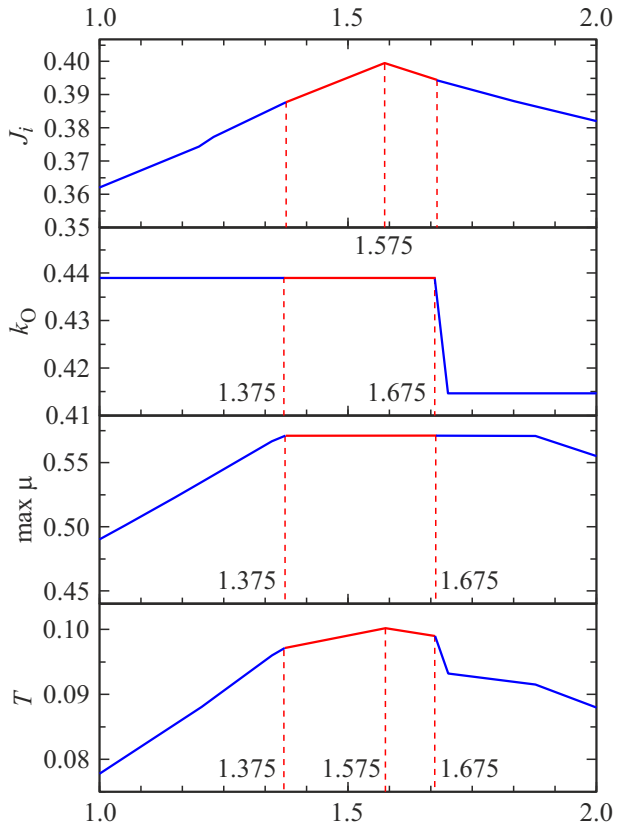

Figure 5. Jaccard index, Oskorbin coefficient k_O, the size of the maximum clique of k_{BG}, the combined measure of compatibility T as per [2].

The value of the argument of point estimate (8) (Fig. 5):

$$k_{BG} = 1.57. \tag{12}$$

The combined measure of compatibility provides an interval estimate

$$k = [1.38, 1.68]. \tag{13}$$

It is clear that the point value k_{BG} is reliably inside the interval estimate $k_{BG} \in k$, so the Jaccard index extremum provides the reliable point estimate.

The graphs of the used measures of compatibility are shown in Fig. 5.

Fig. 5 shows in red the external estimate (12) of the interval multiplicative multiplier taking into account k_{BG}. The resultant measure of compatibilty T [2] exhaustively describes both the external and internal estimates, whereas the optimum internal estimate T coincides with the optimum of the Jaccard interval measure [1]:

$$\arg\max T = \arg\max Ji.$$

Table 2 shows modified data of the columns 2 and 3 of Table 1 taking into account the optimum multiplier k_{BG} (11).

Now let us consider 27 measurements as a single estimate

$$\mathbf{X} = \{\mathbf{X}^p, \mathbf{X}^c\} = \{\mathbf{X}^p, \mathbf{k}_{BG}\mathbf{X}^{c0}\}, \quad i = 1, 2, \ldots, 27. \tag{14}$$

Table 2. Data (1), multiplied by 10^5 (in relation to Table 1 the table has the columns (2) and (3) changed)

№of meas. series	Compton — average	Compton — RSMD	Photopeak	Photopeak — RSMD
(1)	(2)	(3)	(4)	(5)
	x^C	Δx^C	x^p	Δx^p
1	−4.87	4.24	−4.4	2.7
2	−0.31	3.3	−3.4	1.9
3	−6.28	3.3	−6.9	2.4
4	−3.3	3.92	−1.2	2.4
5	−5.81	2.98	−1.0	2.7
6	−2.67	5.81	−10.8	3.5
7	−8.95	4.4	−10.2	2.8
8	−4.4	2.98	−6.3	2
9	−12.56	6.28	−10.4	4.1
10	−3.3	6.12	0.6	3.4
11	−5.65	4.08	−1.8	2
12	−11.3	3.92	−6.6	2.1
13			−4.9	2.1
14			−6.0	2.4
15			−4.0	2.7
Average	−5.5	1.1	−4.8	0.8

The first 15 measurements comply with the initial data $\mathbf{X}^p$. The next 12, starting from the 16-th, comply with the added data $\mathbf{X}^c$. The interval data in $\mathbf{X}^c$ are formed similar to the formula (3) based on the data of the columns 2 and 3 of Table 1. The array of the elementary subintervals $\mathbf{Z} = \{\mathbf{z}_i\}$, $i = 1, 2, \ldots, 53$ is formed similar to $\mathbf{Z}^p$ (4) as per the condition (5).

Let us provide the results of calculation of the interval mode, the maximum clique and the Oskorbin coefficient

$$\operatorname{mode}\mathbf{X} = \mathbf{z}_{24} = [-6.7, -6.3], \tag{15}$$

$$\max\mu_i = 18, \tag{16}$$

$$k_O = 1.7. \tag{17}$$

Fig. 6 shows in red the graph of frequencies for the sample $\mathbf{X}^p$ (3), in grey — the similar graph for $\mathbf{X}^c$, and in blue — for $\mathbf{X}$ (13).

The mode of distribution of $\mathbf{X}^c$ is a multi-interval in the same way as mode $\mathbf{X}^p$ (6):

$$\operatorname{mode}\mathbf{X}^c = [-7.4, -7.4] \cup [-7.2, -6.3]. \tag{18}$$

The interval mode mode $\mathbf{X}$ (14) of the whole sample (13) is an intersection of the intervalsmode $\mathbf{X}^p$ (6)

and mode $\mathbf{X}^c$ (17) and consists of a single elementary subinterval $[-6.7, -6.3]$.

The band scattering diagram of the combined sample $\mathbf{X}$ (14) is shown in Fig. 7. The maximum clique K (18) is highlighted in red.

The numbers of measurements for the maximum clique K of the sample $\mathbf{X}$ (14) are the following:

$$K = K_p + K_C = \{1, 3, 8, 9, 12, 13, 14, 15, 16, 18, 19, 20, 21, 22, 23, 24, 25, 26\}. \quad (19)$$

Here, K_p (9) — the array for the maximum clique of the sample $\mathbf{X}^p$ (4).

It should be noted that of the 12 added measurements 10 are included in the maximum clique (14). Let us note noticeable improvement of the uniformity properties of the sample $\mathbf{X}$ (12) as compared to the sample $\mathbf{X}^p$ (3). The distribution of frequencies of the elementary subintervals became a unimodal one. Correspondingly, the multi-interval of the interval mode mode $\mathbf{X}^p$ (7) became the common interval mode $\mathbf{X}$ (15).

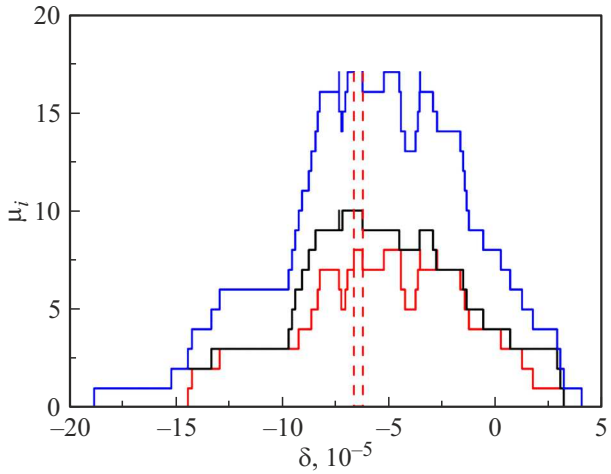

Figure 6. Graph of frequencies of the elementary subintervals $\mathbf{Z}$ of the combined sample $\mathbf{X}$ (11).

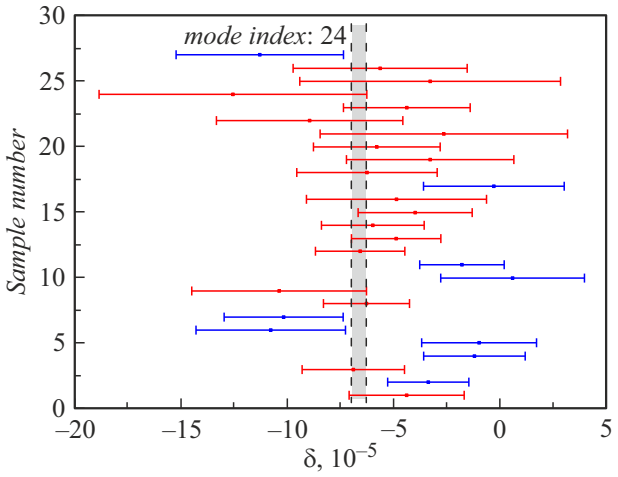

Figure 7. Scattering pattern of the combined sample (Table 2).

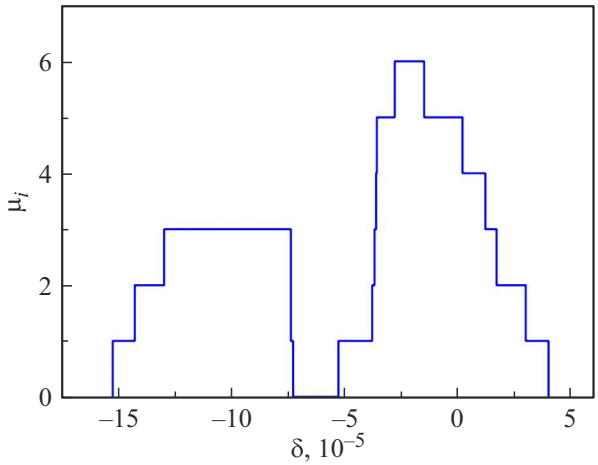

Figure 8. Graph of frequencies of the elementary subintervals Z_{out} for the combined sample $\mathbf{X}$ (14).

It should be noted that the measurements outside the maximum clique (19) as highlighted in blue in Fig. 7 have many non-empty intersections with other elements of the interval sample X. Thus, they should not be included in the invalid ones and considered to be outliers, they are also useful for characterization of the entire data volume [6]. The work [3] contains extensive discussion of in compatible samples and methods of their analysis.

Let us name such measurements outliers (marginal, or outsiders) without any negative meaning of this epithet. Let us denote the set of the outliers as K_{out}:

$$K_{\text{out}} = \{2, 4, 5, 6, 7, 10, 11, 17, 27\}.$$

Let us plot frequencies of the elementary subintervals Z_{out} of outliers of the combined sample $\mathbf{X}$ (11). As it is clear from Fig. 8, the distribution is bimodal and the modes are to the left and to the right of mode $\mathbf{X}$ (14).

The set of the values of $\mathbf{X}(K_{\text{out}})$ is narrower that the maximum clique $\mathbf{X}$ (14):

$$\text{wid}[-15.3, 4.0] = 19.3 < \text{wid}[-18.9, 3.2] = 22.1.$$

It can be also noted that the intervals of the „left“ mode are included in the interval $x_{24} = [-18.9, -6.3]$, so are the majority of the intervals of the „right“ mode — in $x_{21} = [-8.5, 3.2]$. This fact reflects the so-called Khlebnikov paradox [3]: the wider intervals x_{24}, x_{21} are included in the maximum clique, while the narrower intervals $\mathbf{X}(K_{\text{out}})$ are not included therein.

2.3. Discussion of the results

To compare the obtained results with calculation of the physical quantity δ [6], let us calculate by the theory&probabality mathematical statistics as per data of Table 2.

$$\delta_{(P)} = (-4.8 \pm 0.8) \cdot 10^{-5} \text{ [6]},$$

$$P_{\gamma(P)} = (-1.5 \pm 0.3) \cdot 10^{-3} \text{ [6]}; \quad (20)$$

$$\delta_{(C+P)} = (-5.1 \pm 0.7) \cdot 10^{-5},$$

$$P_{\gamma(C+P)} = (-1.6 \pm 0.3) \cdot 10^{-3}, \quad (21)$$

where the index P indicates calculations of the photopeak data and the index $C + P$ corresponds to the same calculations with the data of the photopeak and the Compton spectrum. The uncertainty in the estimate (21) is given for the significance level which corresponds to one standard deviation as in the paper [6].

The results of the calculations (20) show good compliance of the new estimates with the calculations in [6] at slight decrease of the estimates of statistical spread. The results (21) are correction of [6] and they will be separately published together with discussion of nuclear-physics aspects of the task and various calculations.

The proposed method is developed in a more detailed method of data correction within the Compton scattering range. The present work has used the same coefficient (9) for all the measurements. At the same time, the paper [6] provides data on measurement of the background for each measurement. Taking into account the spectra form of the gamma quanta [16], it is possible to calculate the background contribution to the effect individually for all the data of the sample.

Let us now discuss the issue of the status of the interval measurements in a broader context of data analysis. We have taken the basic sample 3 (Table 1) as a starting point of the study and added additional data (after necessary correction) from the same table thereto, which have been not included in the processing. The point estimates and the scattering measures (21) have not varied considerably in relation to the initial ones (20).

But what changes after enhancing a sample power? The number of mutually compatible sample data has substantially increased from 8 of 15 to 18 of 27 (while the number of the outliers has insignificantly increased from 7 to 9). Thus, the result became more representative. This fact indicates that one should more attentively consider the status of the added measurements in terms of the terminology of Section 1.2.

Section 1.2 denote the model-compatible measurements as internal ones which do not participate in formation of the estimates of the information set. It is really so, but the contribution of such measurements to the parameters of the compatibility measures is high, vice versa. Here, the „active" boundary measurements do not contribute decisively. The English terminology denotes this by the terminology pair „inlier/outlier". It is internal measurements that form the interval mode and are included in the maximum clique of the interval sample. The authors of the book [3] have proposed to name the internal measurements „totally compatible".

Conclusion

An original approach of combining the samples is proposed. The approach is based on using the combined measure of compatibility for the samples with the interval uncertainty. As a result, the maximum clique of the data sample is substantially increased. A new value is obtained for the parameter $P\gamma$ — the basic nuclear reaction of neutron capture by a proton. $P\gamma$ is most often used in astrophysical calculations when considering the reverse reaction of photofission of the deuton taking into account polarization of the gamma quanta.

Acknowledgments

The authors would like to thank participants of All-Russian Interval Analysis webinar — S.I. Zhilin, S.I. Kumkov, A.V. Prolubnikov, E.V. Chausova, S.P. Shary — for creative and constructive cooperation in the field of data analysis with interval uncertainty and in terminology formulization, and O.M. Skrekel' — for calculation of the spectra of gamma quanta.

Funding

The section „Practical example" is supported by the state RAS assignment (the RF state assignment FFUG-2024-0034). The section „Information set and measurement status" is supported by the state RAS assignment (the RF state assignment FFUG-2024-0028).

Conflict of interest

The authors declare that they have no conflict of interest.

References

[1] A.N. Bazhenov, A.Yu. Telnova. Meas. Tech., **65** (12), 882 (2023). http://dx.doi.org/10.1007/s11018-023-02180-2
[2] A.N. Bazhenov, S.I. Zhilin, A.Yu. Telnova. Meas. Tech., **11**, 1 (2024). https://doi.org/10.1007/s11018-024-02297-y
[3] A.N. Bazhenov, S.I. Zhilin, S.I. Kumkov, S.P. Sharyi. *Obrabotka i analiz dannykh s interval'noi neopredelennostiyu* (NITs, Regulyarnaya i khaoticheskaya dinamika RKhD, Moskva–Izhevsk, 2024), ISBN 978-5-4344-1018-2 2024 g., 356 s. (in Russian)
[4] S.P. Shary. *Interval'nyi metod obrabotki rezul'tatov mnogokanal'nykh eksperimentov* (Dokt. diss. 01.04.01, Moskva, 2008) (in Russian)
[5] R.B. Kearfott, M.T. Nakao, A. Neumaier, S.M. Rump, S.P. Shary, P. van Hentenryck. *Standardized notation in interval analysis* 2010. Vol. 15. № 1. P. 7–13.
[6] A.N. Bazhenov, L.A. Grigor'eva, V.V. Ivanov, E.A. Kolomensky, V.M. Lobashev, V.A. Nazarenko, A.N. Pirozhkov, Yu.V. Sobolev. Phys. Lett. B, **289** (1–2), 17 (1992).
[7] A.N. Bazhenov, V.M. Lobashev , A.N. Pirozhkov, V.N. Slusar. Nucl. Instrum. Methods Phys. Res., **332** (3), 534 (1993).
[8] A.N. Bazhenov, V.I. Medvedev, A.N. Pirozhkov. Pribory i tekhnika eksperimenta, **4**, 63 (1992). (in Russian)

[9] A.N. Bazhenov, V.V. Ivanov. Nucl. Inst. Methods Phys. Res. A, **337** (2–3), 622 (1994).
[10] V.V. Ivanov, V.A. Solovey. Nucl. Inst. Methods Phys. Res. Section A, **311** (3), 569 (1992).
[11] I.B. Khriplovich. Phys. Atom. Nuclei, **64**, 516 (2001). https://doi.org/10.1134/1.1358476
[12] A.P. Burichenko, 1.B. Khriplovich. Nucl. Phys. A, **515** (1), 139 (1990). https://doi.org/10.1016/0375-9474(90)90327-I
[13] S.P. Shilpashree. Intern. J. Modern Phys. E, **22** (5), 1350030 (2013).
[14] W.M. Snow, A. Bazhenov, C.S. Blessinger, J.D. Bowman, T.E. Chupp, K.P. Coulter, S.J. Freedman, B.K. Fujikawa, T.R. Gentile, G.L. Greene, G. Hansen, G.E. Hogan, S. Ishimoto, G.L. Jones, J.N. Knudson, E. Kolomenski, S.K. Lamoreaux, M.B. Leuschner, A. Masaike, Y. Masuda, Y. Matsuda, G.L. Morgan, K. Morimoto, C.L. Morris, H. Nann, S.I. Penttilä, A. Pirozhkov, V.R. Pomeroy, D.R. Rich, A. Serebrov, E.I. Sharapov, D.A. Smith, T.B. Smith, R.C. Welsh, F.E. Wietfeldt, W.S. Wilburn, V.W. Yuan, J. Zerger. Nucl. Instrum. Methods Phys. Res. A, **440**, 729 (2000). DOI: 10.1016/S0168-9002(99)01071-2
[15] D. Blyth, J. Fry, N. Fomin, R. Alarcon, L. Alonzi, E. Askanazi, S. Baeßler, S. Balascuta, L. Barrón-Palos, A. Barzilov, J.D. Bowman, N. Birge, J.R. Calarco, T.E. Chupp, V. Cianciolo, C.E. Coppola, C.B. Crawford, K. Craycraft, D. Evans, C. Fieseler, E. Frlež, I. Garishvili, M.T.W. Gericke, R.C. Gillis, K.B. Grammer, G.L. Greene, J. Hall, J. Hamblen, C. Hayes, E.B. Iverson, M.L. Kabir, S. Kucuker, B. Lauss, R. Mahurin, M. McCrea, M. Maldonado-Velázquez, Y. Masuda, J. Mei, R. Milburn, P.E. Mueller, M. Musgrave, H. Nann, I. Novikov, D. Parsons, S.I. Penttilä, D. Počanić, A. Ramirez-Morales, M. Root, A. Salas-Bacci, S. Santra, S. Schröder, E. Scott, P.-N. Seo, E.I. Sharapov, F. Simmons, W.M. Snow, A. Sprow, J. Stewart, E. Tang, Z. Tang, X. Tong, D.J. Turkoglu, R. Whitehead, W.S. Wilburn. Phys. Rev. Lett., **121**, 24 (2002).
[16] O.M. Skrekel'. *Chislennoe modelirovanie spektrov gamma-kvantov* (Chastnoye soobshchenie. 2022). (in Russian)

Translated by M.Shevelev